Transcranial Doppler Ultrasonography as a Diagnostic Tool for Head Trauma

Amr AlBakry, Magdy El-Sayed Hassan Rashed, Ahmed Hamouda abdelaziz Mohamed salem, Wael Abd-Elrahman El-Mesallamy

Neurosurgery Department, Faculty of Medicine, Zagazig University

Corresponding author: Ahmed Hamouda abdelaziz Mohamed salem

Email: a.hamoda22@medicine.zu.edu.eg, **Mobile:** 01143897656

Article History: Received: 25.06.2023 **Revised:**09.07.2023 **Accepted:** 23.07.2023

Abstract:

Head trauma (AHT) is the leading cause of fatal head injuries. Transcranial Doppler (TCD) has provided a method of non-invasively monitoring cerebral physiology and has become an invaluable tool in neurocritical care. In this narrative review, we examine the role TCD has in the management of the traumatic brain injury (TBI) patients.

Keywords: Transcranial Doppler Ultrasonography, Head Trauma, Brain Injury.

DOI: 10.53555/ecb/2023.12.1109

Introduction:

Transcranial Doppler (TCD) ultrasonography is a noninvasive ultrasound (US) study, which was introduced in clinical practice in 1982, since then it has been extensively applied on both outpatient and inpatient settings. TCD ultrasonography involves the use of a low-frequency (≤2 MHz) transducer, placed on the scalp, to insonate the basal cerebral arteries through relatively thin bone windows. It is inexpensive, repeatable, and allows continuous bedside monitoring of cerebral blood flow velocity (CBFV), which is particularly useful in the intensive care setting **(1)**

The technique is however highly operator dependent, which can significantly limit its utility. It also has a long learning curve to acquire the three dimensional understanding of cerebrovascular anatomy necessary for competency. Furthermore, approximately 10–20% of patients have inadequate transtemporal acoustic windows **(2).**

TCD has important clinical application in the management of patients with sickle-cell disease, brain stem death, and raised intracranial pressure (ICP). Moreover TCD allows for

intraoperative monitoring, evaluation of vasomotor function and assessment of cerebral micro embolism due to right to left cardiac shunts **(3).**

Other clinical applications of TCD include monitoring of cerebral circulation and embolization during cardiopulmonary bypass, carotid end arterectomies, and carotid artery stenting **(1).**

Combined with waveform morphology, indices derived from flow velocity readings such as Gosling's pulsatility index (PI) and the Lindegaard ratio (LR) allow identification of increased cerebrovascular resistance, vasospasm and hyperdynamic flow states, which characterize the above clinical conditions **(2).**

Anatomy of Main Intracranial Arteries

For better understanding of TCD findings and its applications in clinical setting, can be useful to make a brief description of the anatomy of intracranial arteries of major clinical interest: Internal carotid artery (ICA), middle cerebral artery (MCA), anterior cerebral artery (ACA) and posterior cerebral artery (PCA) as in figure (1) **(4).**

The ICA, together with the external carotid artery is the terminal branch of the common carotid artery. It starts at C3 and C5 vertebral level, and it has been sub-divided into seven segments (named from C1 to C7): (1) cervical segment; (2) petrous (horizontal) segment; (3) lacerum segment; (4) cavernous segment; (5) clinoid segment; (6) ophthalmic (supraclinoid) segment; and (7) communicating (terminal) segment. The ICA gives rise to two terminal branches which are the MCA and the ACA **(5).**

The carotid siphon is an S-shaped part to the ICA radiologically used and divided into five segments: C1 (terminal ICA segment), C2 (upper carotid siphon), C3 (carotid knee), C4 (inferior carotid siphon) and C5 (precavernous/ganglionic segment) as in figure (2)**(6).**

The MCA is the most frequently insonated artery during TCD examinations. It arises from the ICA and runs into the lateral sulcus where it then branches and gives blood to many parts of the lateral cerebral cortex as in figure (3). It can be subdivided into 4 tracts. The sphenoidal segment, M1 is also called the horizontal segment, because of its origin and its lateral course on sphenoid bone. The insular segment, M2 segment, is situated anteriorly on the insula. The opercular segments, M3 segment, extend laterally and exteriorly from the insula towards the cortex. The Cortical segments, the M4 terminal segments, irrigate cortex **(1).**

The ACA is smaller than MCA, and arches anteromedially to run anterior to genu of the corpus callosum, where the artery divides into its two major branches, pericallosal and callosomarginal **(7).**

the ACA is divided into two segments: A1 (precommunicating segment) and A2 (postcommunicating segment)**(8).**

The PCA represents the terminal branches of the basilar artery (BA) and irrigate the occipital lobes and posteromedial temporal lobes **(1).**

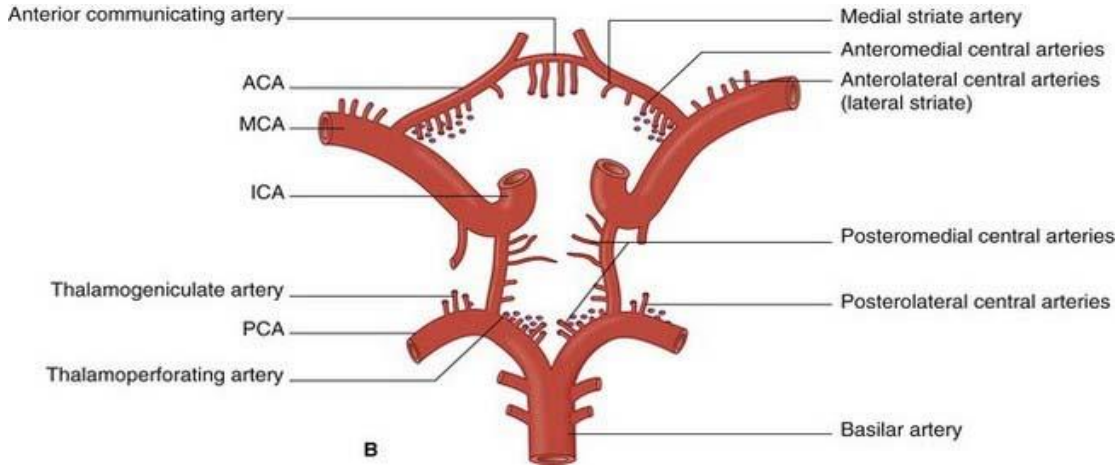

Fig (1): The arteries comprising the circle of Willis **(9).**

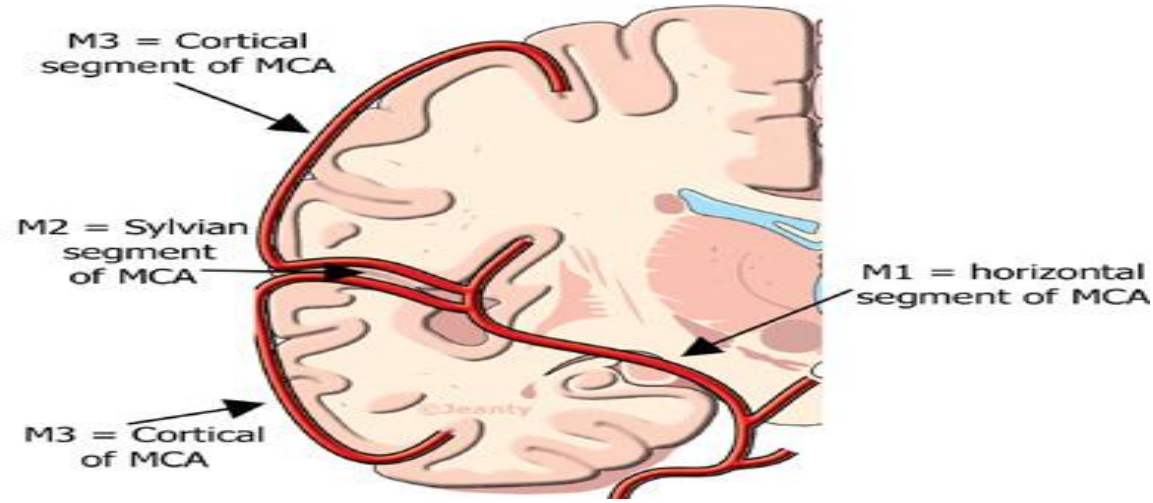

Fig (2): shows M1, M2 and M3 segments of the middle cerebral artery **(10)**

The (PCA) is divided into four segments: P1 (precommunicating segment), P2 (postcommunicating segment), P3(quadrigeminal segment), and P4 (calcarine segment).

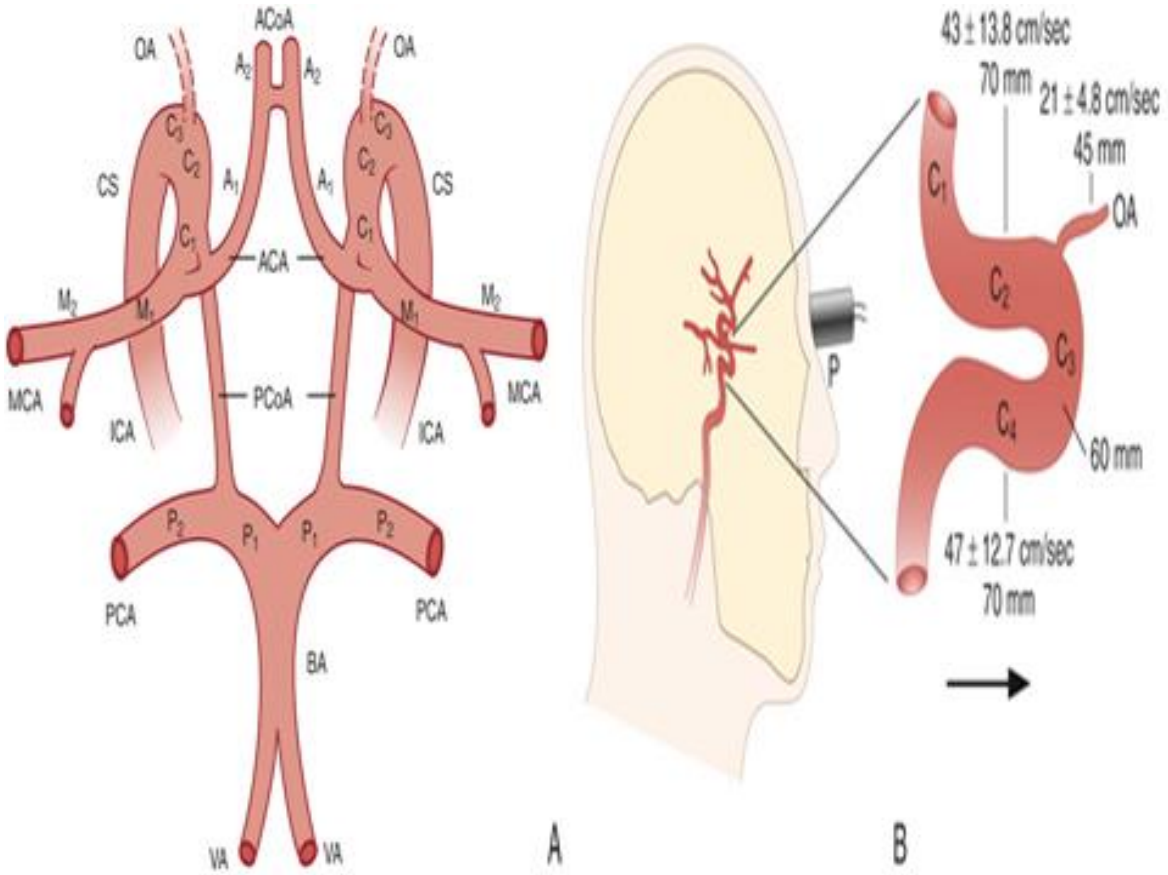

Fig (3): shows segments of anterior and posterior cerebral arteries besides carotid siphon **(11).**

PROBE AND SCANNING PROCEDURES

In clinical practice the most frequently used transducer is a pulsed Doppler sectorial probe with a 2.0-3.5 MHz emission frequency capable of changing the size of the sample volume in order to adapt to the diameter of major intracranial arteries, moreover the angle and position of insonation should be adjusted to provide/determinated the highest quality Doppler signal **(1).**

TCD can be conducted using two acquisition modalities. The first is transcranial color-coded duplex sonography (TCCS), in which it is displayed a two-dimensional color coded image and, once the desired blood vessel is insonated, blood flow velocities may be measured using pulsed wave (PW) Doppler. The second method is conventional TCD, using only Doppler probe function **(12).**

The TCDS with combined Color Flow and power Doppler provides more useful data than TCD since it allows direct imaging of the intracranial arteries, their anatomic course, diameter and relationships with the adjacent structures. Although the use of TCCS can be considered superior

to TCD, no substantial differences were found when the two methods were compared in their accuracy to detect vasospasm in the setting of acute subarachnoidal hemorrhage (SAH) **(1).**

In order to get a better quality of the Doppler signal in spite of background noises, the TCD devices are equipped with a larger sample volume compared to other PW Doppler probe. Specific Doppler settings used in TCD examination include also the emission power between 10 and 100 mW/cm2/second and a pulse repetition frequency (PRF) up to 20 kHz with a focus depth between 40 and 60 mm **(1).**

ACOUSTIC WINDOWS AND SCANNING PLANE

As can been shown in figure (4) there are four acoustic windows that can be employed for TCD **(13).**

In general terms transcranial United States study is performed using two main scanning planes: The axial and coronal planes at a depth that allows to display also the contralateral vessels (14-16 cm depth), with the brain stem structures remaining in the middle of the scanning plane **(1).** The coronal scan is obtained by rotating the probe of 90° from the axial position. In this view are shown the third ventricle, the lateral ventricles, the thalamus and internal capsule. The examination carried out on this plane is mainly useful for assessment of the shift of the median line caused by space occupying lesions (ischaemic area, haemorrhage and tumors) **(1).**

The axial scan is the one most commonly used and it allows two different types of imaging planes: The mesencephalic and diencephalic views. The mesencephalic plane is obtained by positioning the probe parallel to the zygomatic arch. At this level can be identified the hypoechogenic “butterfly-shaped midbrain”, located about half of the scanning plane. In the 75% of cases, can be also detected the posterior communicating arteries if they have enough relevant diameter. In the middle of the diencephalic plane, which is obtained by slightly tilting the transducer 10 degrees upwards, can be seen the III ventricle: Behind it can be identified hyperechogenic pineal gland, while the thalamus and internal capsule are located anteriorly to it. The lateral ventricles can be also detected **(14).**

Fig (4): Four acoustic windows commonly used in transcranial Doppler examination: transtemporal window (A), submandibular window (B), transorbital window (C), suboccipital window (D) **(15).**

The temporal window is situated above the zygomatic arch, anterior to the tragus, using an axial plane in order to obtain a mesencephalic view, with the patient's head in the antero-posterior position. This window can be divided in an anterior, middle and posterior zone and allows to identify the MCA, in particular M1 and M2 tracts as in figure (5). From this approach can be also visualized A1 segment of the ACA, P1 and P2 segments of the PCA and C1 segment of the carotid siphon (CS). In this temporal view can be also seen the communicating arteries (anterior and posterior) and the distal end of the BA **(16).**

It should be noted that about 10%-20% of subjects have poor and unsuitable trans-temporal acoustic views, depending on patient age, female sex, and other factors affecting the temporal bone thickness **(17).**

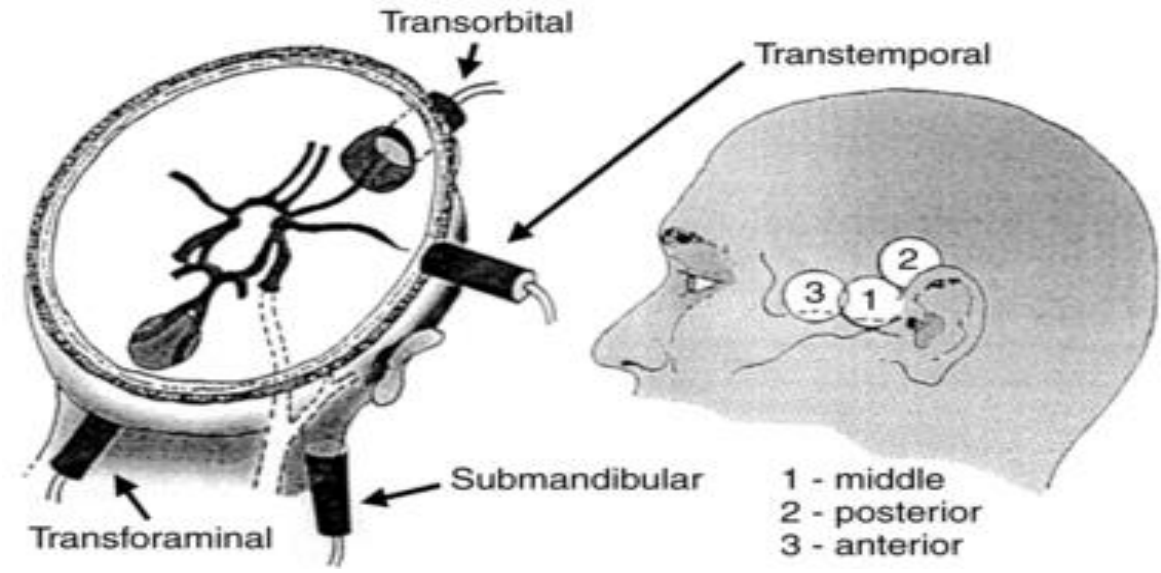

Fig (5): Four windows of transcranial Doppler insonation *(left image, clockwise):* orbital, temporal, submandibular, and foraminal. The temporal window has three aspects *(right image):* 1-middle; 2- posterior; 3- anterior **(18).**

In the occipital window, the probe must be positioned on the median sub-occipital line and the patient should be sitting or lying down with the head turned to opposite direction respect to the operator with the chin lowered toward the shoulder. With US beam passing through the foramen magnum in this window it can be visualized the intracranial segment of the two vertebral arteries (VA) and the basilar trunk. All these three vessels dispose in a Y shape with their flow, depicted in blue color, moving away from the probe. In this view, with slight lateral movements it is possible to display also the inferior cerebellar arteries, the posterior and the anterior **(1).**

The submandibular window is used only for detecting the terminal segment (C5-C6) of the internal carotid artery (distal extradural parts). This approach is can be useful in those cases in which the absence of other "windows" precludes a more complete hemodynamic assessment of the Circle of Willis **(14).**

The orbital window, transducer is put perpendicularly to the eyelid, with patient's eye closed and looking on the opposite side respect to the probe. This approach allows to insonate the ophthalmic artery and the C2, C3 and C4 segments of the carotid syphon, through the foramen of the ocular cavity. The limitation of this approach is represented by the potential retinal injuries caused by the US beam: It is advisable to reduce 10%-15% power of the device respect to transtemporal scan **(1).**

In fact the most frequently examined intracranial vessel in clinical practice is the MCA, it is easily delineated through the temporal window above the zygomatic arch. The 60%-70% of the

ICA blood flow is directed to MCA, so its TCD evaluation can be taken to represent almost total blood flow to ipsilateral hemisphere. MCA is detected at a depth of 45-60 mm, and the blood flow is directed toward the probe**(19).**

The identification of the sphenoid bone, through the "butterfly wing sign", leads to an easy MCA visualization in almost all patients, with a constant depth of 59 ± 3 mm. The time to achieve an adequate echographic image of MCA is about 50 ± 20 **(20)**

TCD: PHYSICAL PRINCIPLES AND TCD INDICES

Theta (θ) is the angle of insonation or the angle of the emitted wave relative to the direction of vessel (blood flow). If the angle is zero, or the emitted wave is parallel to the direction of flow, the cosine of zero is 1, and we have achieved the most accurate measure of flow velocity as been shown in figure (6). The larger the angle, the larger is the cosine of the angle; hence, the greater is the error in our velocity measure. Therefore, it is important to minimize this angle to less than 30 degrees to keep the error below 15% **(15).**

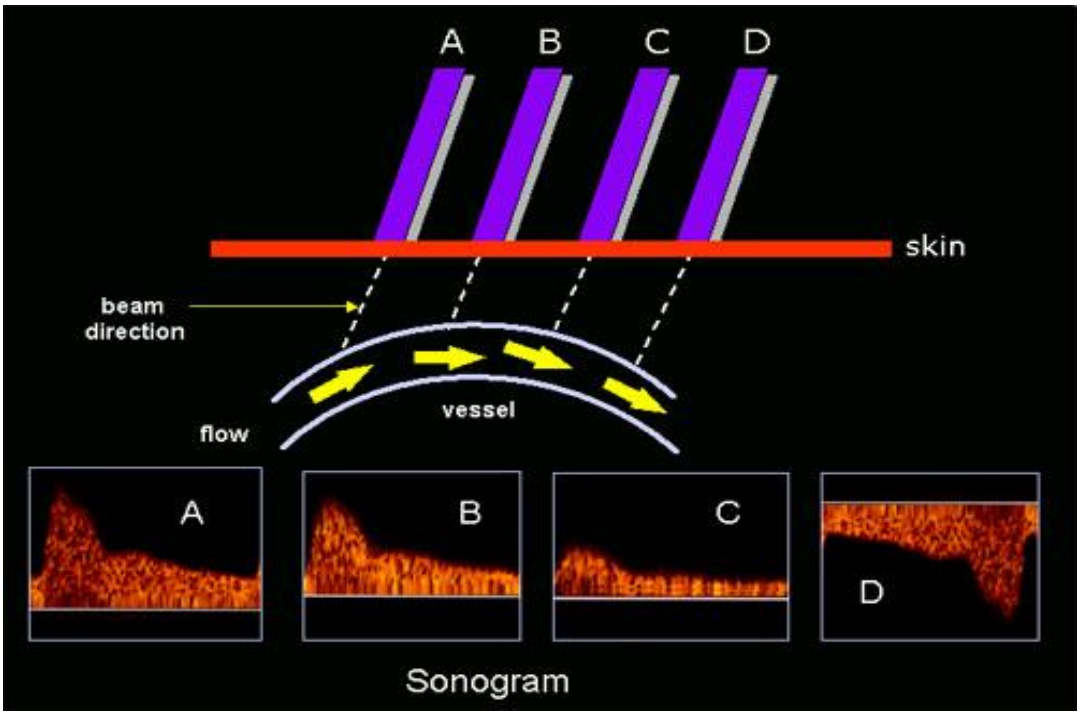

Fig (6): Effect of the Doppler angle in the sonogram. **(A)** higher-frequency Doppler signal is obtained if the beam is aligned more to the direction of flow. In the diagram, beam **(A)** is more aligned than **(B)** and produces higher-frequency Doppler signals. The beam/flow angle at **(C)** is almost 90° and there is a very poor Doppler signal. The flow at **(D)** is away from the beam and there is a negative signal **(21).**

TCD examination is executed placing on the surface of the skull a probe of a range-gated ultrasound Doppler instrument, which allows to determine flow velocities in the intracranial arteries. The attenuation of US beam due to bone and soft tissues requires a low emission frequency in order to provide satisfactory recordings of intracranial CBFVs, usually a 2-MHz frequency is adopted **(22).**

The transmission of an ultrasound beam through skull is influenced by structural characteristics of the diploe bone: The almost complete absence of bone spicules makes penetration of the ultrasound similar to conventional "acoustic windows" consenting the visualization of intracranial vessels. First of all the patient should be lying in supine position, with his head and shoulders on a pillow **(1).**

M-mode Doppler had the advantage of simultaneously displaying the intensity and direction of intracranial blood flow with over 6 cm or more of intracranial space, which simplified the examination technique as in figure (7) and (8) **(23).**

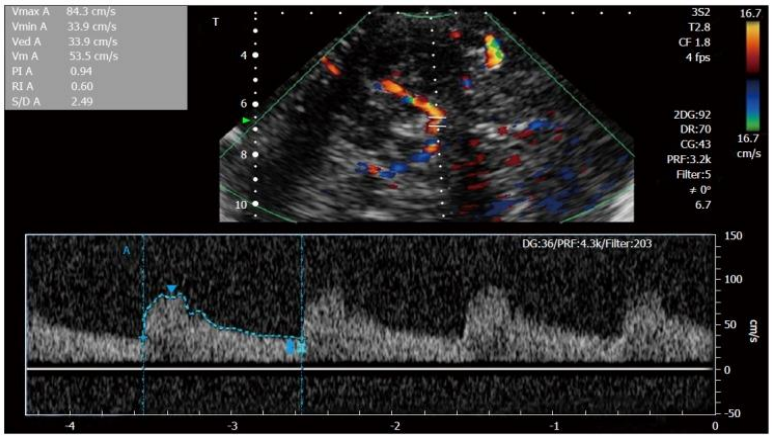

Fig (7): Transcranial Doppler spectral Doppler study of intracranial middle cerebral artery **(1).**

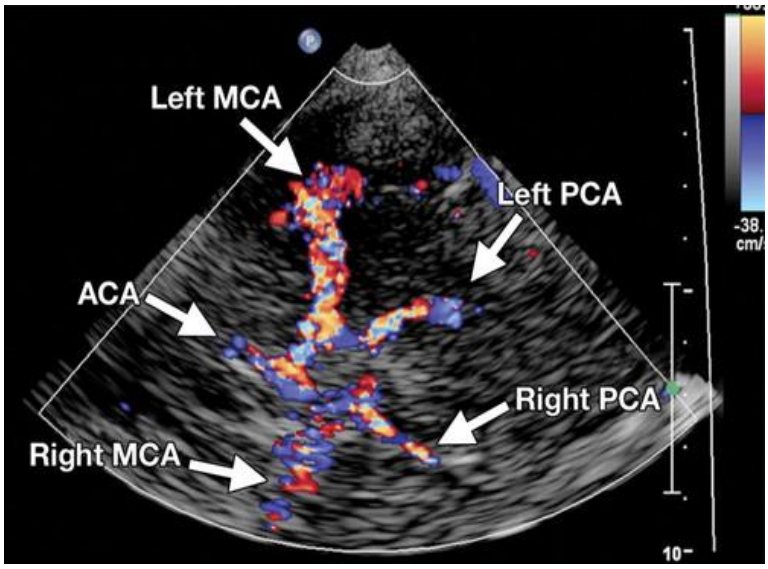

Fig (8): Color Doppler flow image obtained with a transtemporal window shows blood flow through the circle of Willis **(24)**

TCD Indices

Peak systolic velocity (PSV in cm/s*)* is the first peak on a TCD waveform from each cardiac cycle. A rapid upstroke represents the absence of a severe stenotic lesion between the insonated intracranial arterial segment and heart **(23).**

End diastolic velocity (EDV in cm/s) lies between 20 and 50% of the peak systolic velocity (PSV) values, indicating a low resistance intracranial arterial flow pattern, seen in all major intracranial arteries **(23).**

Mean flow velocity (MFV in cm/s) is a central parameter in TCD and is equal [PSV + (EDV × 2)]/3. When MFV is increased, it may indicate stenosis, vasospasm, or hyper dynamic flow. A decreased value may indicate hypotension, decreased CBF, ICP, or brain stem death. Focal arterial stenosis or vasospasm is represented by an increased MFV within a 5–10 mm segment, usually by > 30 cm/s compared with the asymptomatic side **(2)**

According to **(25)** a number of physiological factors may influence MFV. , as described in Table (1).

Table (1): Factors influencing MFV **(25):**

Age	Increases up to 6–10 years of age then decreases
Sex	Higher MFV in women than men
Pregnancy	Decreased in the 3rd trimester
PCO2	Increases with increasing PCO2
Mean arterial Pressure(MAP)	Increases with increasing MAP (CBF auto regulates between CPP 50–150 mmHg)
Hematocrit	Increases with decreasing hematocrit

The normal parametrs of the individual intracranial vessels are showed in Table (2).

Table (2): Normal parameter of the individual intracranial vessels **(4):**

Artery	**Window**	**Depth (mm)**	**Direction**	**Mean Flow Velocity**
MCA	Temporal	30 to 60	Toward probe	55 ± 12 cm/s
ACA	Temporal	60 to 85	Away	50 ± 11 cm/s
PCA	Temporal	60 to 70	Bidirectional	40 ± 10 cm/s
TICA	Temporal	55 to 65	Toward	39 ± 09 cm/s
ICA (siphon)	Orbital	60 to 80	Bidirectional	45 ± 15 cm/s

OA	Orbital	40 to 60	Toward	20 ± 10 cm/s
VA	Occipital	60 to 80	Away	38 ± 10 cm/s
BA	Occipital	80 to 110	Away	41 ± 10 cm/s

According to **Kassab et al., (4)** basic Observations Regarding Blood FVs and PI in Different Vascular Scenarios**:**

- Pure focal narrowing at the site of insonation will cause an increase in FV.
- Narrowing or obstructing lesions proximal to the insonation site will cause a decrease in FV observed at the insonation site.
- Downstream (distal) decrease in vascular resistance (as in the presence of arteriovenous malformation will increase FV and decrease PI at the site of insonation.
- Downstream increased vascular resistance (as in stenosis or obstruction) will decrease FV and increase PI proximal to lesion.

Pulsatility index (PI*)* provides information on downstream cerebral vascular resistance and is equal to (PSV-EDV)/MFV. PI is normally 0.5 to 1.19 and independent of the angle of insonation **(26)**

Proximal stenosis or occlusion may lower the PI below 0.5 due to downstream arteriolar vasodilation whilst distal occlusion or constriction may increase the PI above 1.19. PI less than 0.5 may indicate an arterio venous malformation as vessel resistance in proximal vessels is reduced due to continuous distal venous flow **(2).**

Resistance index (RI) is equal to (PSV-EDV)/PSV with values > 0.8 indicating increased downstream resistance. Derangements of RI reflect similar disease patterns as observed with an abnormal PI **(27).**

Systolic diastolic ratio (S/D) represents the ratio between PSV and EDV. This is not used for clinical purposes **(23).**

The Lindegaard ratio (LR) permits to differentiate between hyperdynamic arterial blood flow and vasospasm as in table (3). It is obtained by the following equation **(1)**:

(LR = MCA mean CBFV/extra cranial ICA mean CBFV).

This ratio tends to increase in relation to the severity of symptomatic vasospasm (VSP). Normal reference range is from 1.1 to 2.3 and in the absence of vasospasm is lower than 3**(28)**

When the CBFV is elevated but the LR ratio is lower than 3, the elevation is considered to be caused by hyperemia, in case of a ratio more than 6, there is a severe VSP **(19).**

Moreover, for detecting the severity of BA vasospasm it is calculated the modified LR: BA means CBFV/left or right extracranial VA Mean CBFV; modified LR: 2 to 2.49 possible VSP; LR modified: 2.5 to 2.99 moderate VSP; LR modified: > 3 severe VSP **(1)**.

Table (3): Grading of vasospasm severity **(29):**

Degree of MCA or ICA vasospasm	**MFV (cm/s)**	**LR**
Mild (<25%)	120–149	3–6
Moderate (25–50%)	150–199	3–6
Severe (>50%)	>200	>6
Degree of BA vasospasm	**MFV (cm/s)**	**Modified LR**
May represent vasospasm	70–85	2–2.49
Moderate (25–50%)	>85	2.5–2.99
Severe (>50%)	>85	>3

Specialist Indices

Vasodilatory stimulation via breath holding and CO2-induced hypercapnia can detect an impaired cerebral vasomotor reserve (VMR) and impending stroke **(2).**

The breath-holding index (BHI) is equal to ((CBFV max − CBFV min)/time of breath hold) ×100. A BHI >0.6 is normal; between 0.21 and 0.60 is impaired VMR, whilst ≤0.20 is significantly impaired VMR **(30)**

The CO2 challenge VMR index is calculated using the average CBF-V at baseline, during hypercapnia and hypocapnia, and is equal to (Hypercapnia CBF-V − Hypocapnia CBF-V) / (Baseline CBF-V) × 100. A value greater than 70% is normal, 39–69% is mild to moderately reduced VMR, 16–38% is severely reduced VMR, and ≤15% is exhausted VMR **(2).**

TCD in Subarachnoid Hemorrhage

The delayed vasospasm of the cerebral vasculature is angiographically proven in up to 70% of cases of SAH and usually occurs 4 to 17 days after hemorrhageas in figure (9) .The pathogenesis is unclear but is thought to involve the breakdown of blood in the subarachnoid space and secondary cellular mechanisms which culminate in vasoconstriction of adjacent intracranial arteries **(31)**

Angiography is the gold standard for detecting vasospasm but is an invasive technique and unsuited to dynamic monitoring. TCD, however, is non-invasive, portable, and able to dynamically assess vasospasm and monitor the effectiveness of intervention including triple-H therapy (hypertension, haemodilution, and hypervolaemia), transluminal balloon angioplasty, or pharmacologic vasodilation **(2).**

TCD identifies MCA and BA vasospasm with a high sensitivity and specificity. However, for vasospasm of the ACA and PCA sensitivity of TCD is not inferior **(32)**

Despite the high sensitivity that may be achieved for MCA and BA vasospasm, the prognostic ability of TCD and potential to improve outcome in SAH are challenged. In a cohort of 580 SAH patients, only 84% of those with delayed cerebral ischemia (DCI) had evidence of angiographic vasospasm. Furthermore, DCI, and not vasospasm, was significantly associated with adverse outcome. This may be due to additional pathogenic mechanisms such as reperfusion injury, hydrocephalus, and a disrupted blood-brain barrier contributing to neurological decline **(33).**

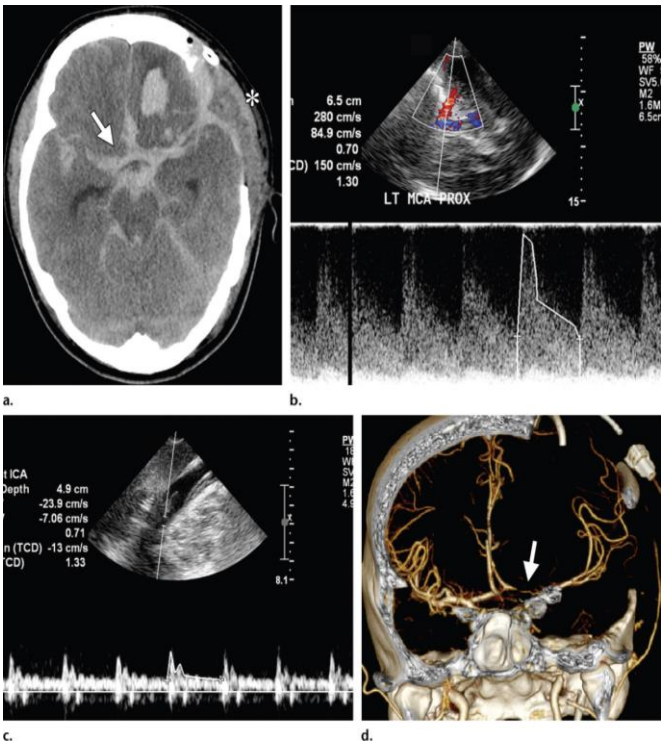

Fig(9): a) Unenhanced axial CT scan of the brain depicts a subarachnoid hemorrhage (arrow) secondary to a ruptured aneurysm. Note the left frontal craniectomy (*****). **(b, c)** Doppler US images and spectral waveforms obtained in the left MCA **(b)** and ipsilateral distal ICA **(c)** show only mildly increased PSV and MFV in the left MCA (280 cm/sec and 150 cm/sec, respectively) but a markedly elevated Lindegaard ratio of 11.5, a finding indicative of severe vasospasm. **(d)** Three-dimensional reconstruction from CT angiography depicts a severe stenosis of the left MCA (arrow) **(24).**

TCD and Raised Intracranial Pressure

Traumatic brain injury (TBI) may lead to hypoperfusion (day 0), hyperemia (days 1–3), vasospasm (days 4–15), and raised ICP. TCD can noninvasively identify such complications and provide prognostic information **(34)**

According to **(35)** doppler sonograms obtained in this model of progressive intracranial hypertension showed four characteristic flow patterns in the following sequence as in figure (10)**:**

- Sharp wave (SW): A progressive increase in ICP brings about a more rapid reduction in flow velocity in the diastolic phase than in the systolic phase, resulting in pronounced pulsatility between peak systole and end of diastole.
- Systolic flow (SF): Following a further rise in ICP, the diastolic part of the flow velocity spectrum starts to disappear.
- Systolic spike (SS): Further elevation of ICP diminishes the waveform, resulting in a brief peak in systole.
- No flow (NF): At the final stage of intracranial hypertension, Doppler signals were not detected at all.

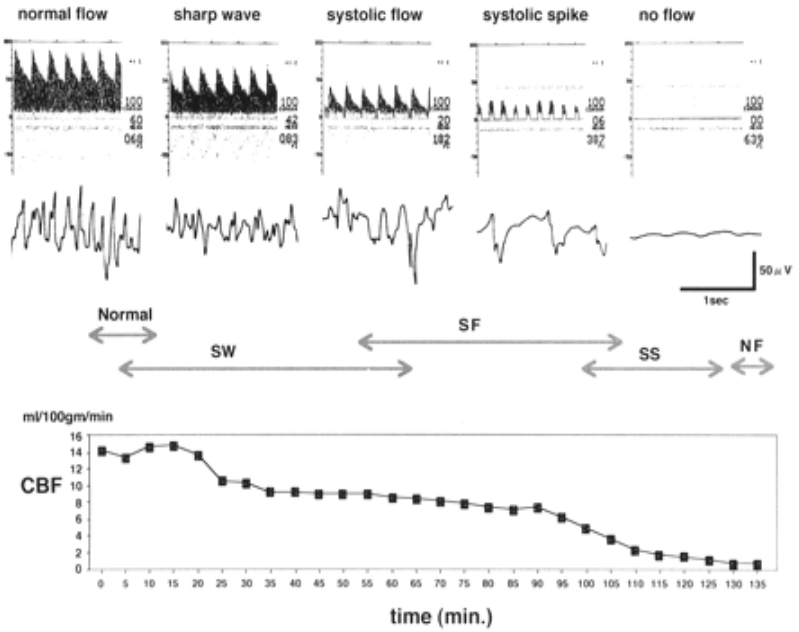

Fig (10): Sequential changes in flow pattern, Electrocorticography (ECoG), and CBF **(35).**

References:

1. D'Andrea, A., Conte, M., Cavallaro, M., Scarafile, R., Riegler, L., Cocchia, R., . . . Santoro, G. J. W. J. o. C. (2016). Transcranial Doppler ultrasonography: From methodology to major clinical applications. 8(7), 383.
2. Naqvi, J., Yap, K. H., Ahmad, G., & Ghosh, J. (2013). Transcranial Doppler ultrasound: a review of the physical principles and major applications in critical care. International journal of vascular medicine, 2013.
3. Reuter-Rice, K. (2017). Transcranial Doppler ultrasound use in pediatric traumatic brain injury. Journal of radiology nursing, 36(1), 3-9.
4. Kassab, M. Y., Majid, A., Bakhtar, O., Farooq, M. U., Patel, K., & Bednarczyk, E. M. (2007). Transcranial Doppler measurements in migraine and nitroglycerin headache. The Journal of headache pain 8, 289-293.
5. Loomis, A. L., & Chakko, M. N. (2022). Doppler trans-cranial assessment, protocols, and interpretation. In StatPearls [Internet]: StatPearls Publishing.
6. Vijaywargiya, M., Deopujari, R., & Athavale, S. A. (2017). Anatomical study of petrous and cavernous parts of internal carotid artery. Anatomy cell biology 50(3), 163-170.
7. Du Toit, F. (2015). Circulus arteriosus cerebri: Anatomical variations and their correlation to cerebral aneurysms. University of Cape Town,
8. Cilliers, K., & Page, B. J. J. T. N. (2016). Review of the anatomy of the distal anterior cerebral artery and its anomalies. 26(5), 653-661.
9. Piechna, A., & Cieślicki, K. J. S. R. (2023). Influence of hydrodynamic and functional nonlinearities of blood flow in the cerebral vasculature on cerebral perfusion and autoregulation pressure reserve. 13(1), 6229.
10. Das, M., Pankaj, P., Jahan, S. J. J. o. E. o. M., & Sciences, D. (2016). A study of insular segment of middle cerebral artery in Northern India. 5(64), 4582-4588.
11. Sander, D., & Widder, B. J. D. s. o. t. b.-s. a. (2022). Carotid Artery. 139.
12. Aleem, I., & Chau, T. J. J. o. n. e. (2012). Towards a hemodynamic BCI using transcranial Doppler without user-specific training data. 10(1), 016005.
13. Wan, Y., Teng, X., Li, S., & Yang, Y. J. F. i. A. N. (2022). Application of transcranial Doppler in cerebrovascular diseases. 14, 1035086.

14. Antignani, P., Benedetti-Valentini, F., Aluigi, L., Baroncelli, T., Camporese, G., Failla, G., . . . Rispoli, P. J. I. A. (2012). Diagnosis of vascular diseases. Ultrasound investigations--guidelines. 31(5 Suppl 1), 1-77.
15. Purkayastha, S., & Sorond, F. (2012). Transcranial Doppler ultrasound: technique and application. Paper presented at the Seminars in neurology.
16. Rodríguez, C. N., & Pugin, D. J. N. i. c. c. m. t. n. i. o. t. c. p. (2022). Neurosonology in ICU: transcranial color-coded duplex sonography (TCCS) protocol. 251-281.
17. Lau, V. I., & Arntfield, R. T. J. C. U. J. (2017). Point-of-care transcranial Doppler by intensivists. 9, 1-11.
18. Saqqur, , M., Khan, , K., Derksen, , C., . . . , A. (2018). Transcranial Doppler and transcranial color duplex in defining collateral cerebral blood flow. Journal of Neuroimaging, 28(5), 455-476.
19. Rasulo, F. A., Calza, S., Robba, C., Taccone, F. S., Biasucci, D. G., Badenes, R., . . . Dibu, J. R. J. C. C. (2022). Transcranial Doppler as a screening test to exclude intracranial hypertension in brain-injured patients: the IMPRESSIT-2 prospective multicenter international study. 26(1), 1-12.
20. Paulus, J., Cinotti, R., Hamel, O., Buffenoir, K., Asehnoune, & Karim. (2014). The echographic “butterfly wing” aspect of the sphenoid bone is a critical landmark to insonate the middle cerebral artery. Intensive care medicine, 40, 1783-1784.
21. Deana, Cristian, Vetrugno, , L., Stefani, , F., ... (2022). Transcranial Doppler in a child: A most valuable imaging modality. Ultrasound, 30(2), 167-172.
22. Greke, C., Neulen, A., Kantelhardt, S. R., Birkenmayer, A., Vollmer, F. C., Thiemann, I., & Giese, A. J. J. o. N. A. (2013). Image-guided transcranial Doppler sonography for monitoring of defined segments of intracranial arteries. 25(1), 55-61.
23. Bathala, Lokesh, Mehndiratta, , M. M., Sharma, & , V. K. (2013). Transcranial doppler: Technique and common findings (Part 1). Annals of Indian Academy of Neurology 16(2), 174.
24. Kirsch, D, J., Mathur, Mahan, Johnson, H, M., . . . , L. M. J. R. (2013). Advances in transcranial Doppler US: imaging ahead. Radiographics, 33(1), E1-E14.
25. Schatlo, B., & Pluta, R. M. J. R. o. r. c. t. (2007). Clinical applications of transcranial Doppler sonography. 2(1), 49-57.

26. Caldiera, , V., Caputi, , L., Ciceri, & Elisa. (2016). Doppler imaging: basic principles and clinical application. Intraoperative Ultrasound in Neurosurgery: From Standard B-Mode to Elastosonography, 101-120.
27. Tsivgoulis, G., Alexandrov, A. V., & Sloan, M. A. (2009). Advances in transcranial Doppler ultrasonography. Current neurology and neuroscience reports, 9(1), 46-54.
28. Lindegaard, K-F, Nornes, H, Bakke, SJ, . . . , P. (1988). Cerebral vasospasm after subarachnoid haemorrhage investigated by means of transcranial Doppler ultrasound. Paper presented at the Proceedings of the 8 th European Congress of Neurosurgery Barcelona, September 6–11, 1987: Intraoperative and Posttraumatic Monitoring and Brain Protection—Cerebro-vascular Lesions—Intracranial Tumours—Benign lntracranial Cystic Lesions, Hydrocephalus, CSF-Volumes—Central Pain Syndromes.
29. Sviri, E, G., Ghodke, B., Britz, G. W., Douville, C. M., Haynor, D. R., . . . Newell, D. W. J. N. (2006). Transcranial Doppler grading criteria for basilar artery vasospasm. 59(2), 360-366.
30. Nicoletto, H. A., & Boland, L. S. J. A. j. o. e. t. (2011). Transcranial Doppler series part v: specialty applications. 51(1), 31-41.
31. Rigamonti, Andrea, Ackery, , A., Baker, Andrew, & Anesthesia, C. J. o. (2008). Monitorage par Doppler transcrânien lors d'une hémorragie sous-arachnoïdienne: un outil indispensable aux soins intensifs. Canadian Journal of Anesthesia, 55, 112-123.
32. Sloan, M., Alexandrov, A., Tegeler, C., Spencer, M., Caplan, L., Feldmann, E., . . . Babikian, V. J. N. (2004). Assessment: Transcranial Doppler ultrasonography:[RETIRED] Report of the Therapeutics and Technology Assessment Subcommittee of the American Academy of Neurology. 62(9), 1468-1481.
33. Jabbarli, R., Pierscianek, D., Rölz, R., Darkwah Oppong, M., Kaier, K., Shah, M., . . . Beck, J. J. N. (2019). Endovascular treatment of cerebral vasospasm after subarachnoid hemorrhage: more is more. 93(5), e458-e466.
34. Razumovsky, Alexander, & (2023). Transcranial Doppler Ultrasound Role for Patients with Traumatic Brain Injury. Journal of Neurosonology Neuroimaging 15(1), 24-37.
35. Nagai, Hidemasa, Moritake, Kouzo, Takaya, Mikio, & Stroke, J. (1997). Correlation between transcranial Doppler ultrasonography and regional cerebral blood flow in experimental intracranial hypertension. 28(3), 603-608.